ACADEMIC PRESS

Available online at www.sciencedirect.com
SCIENCE DIRECT®

Journal of Colloid and Interface Science 259 (2003) 301–308

JOURNAL OF Colloid and Interface Science

www.elsevier.com/locate/jcis

Drag force on a porous, non-homogeneous spheroidal floc in a uniform flow field

Jyh-Ping Hsu * and Yu-Heng Hsieh

Department of Chemical Engineering, National Taiwan University, Taipei 10617, Taiwan, ROC

Received 14 May 2002; accepted 5 November 2002

Abstract

The force acting on a porous spheroidal floc having a nonhomogeneous structure in a uniform flow field is evaluated theoretically. Here, the floc is simulated by an entity having a two-layer type of structure, and its porous nature is mimicked by varying the relative magnitudes of the permeabilities of its inner and outer layers. The results of numerical simulation reveal that, for the same volume-averaged permeability, the drag coefficient of a spheroidal floc with a nonhomogeneous structure is much larger than that of a floc with a homogeneous structure for both prolate and oblate spheroids. This is true regardless of the relative magnitudes of the permeability of the inner layer and that of the outer layer. While the drag coefficient of a homogeneous prolate is the same as that of a homogeneous oblate the drag coefficient of a nonhomogeneous prolate is larger than that of a nonhomogeneous oblate. For the same volume-averaged size, the more nonhomogeneous the structure of a spheroidal floc the easier for the relation between the drag coefficient and the Reynolds number to deviate from a Stokes-law-like relation. For a fixed volume-averaged permeability, the effective drag coefficient increases with the increase in the ratio (polar radius of inner layer/polar radius of floc), regardless of whether its inner layer is less permeable than its outer layer or not.
© 2003 Elsevier Science (USA). All rights reserved.

Keywords: Spheroidal floc; Non-homogeneous porous structure; Drag force; Two-layer model

1. Introduction

The evaluation of the hydrodynamic drag force on the floc formed in a wastewater treatment process exerted by the surrounding fluid is an important problem. Unfortunately, due to the fact that a floc usually has an irregular shape and a highly porous and complicated, essentially random structure, the problem under consideration is nontrivial, in general. Li and Ganczarczyk [1], for example, found that activated sludge floc contains solid particles and a randomly distributed mixture of colloids, organic polymers, and microorganisms, which implies that it has a highly porous and nonuniform structure. Many researchers have studied the behavior of a floc in a flow field. Lee et al. [2] investigated the permeability of spherical flocs containing either spherical or fibrous primary particles. On the basis of Darcy and Brinkman's law for permeability, Adler [3] evaluated the streamlines for the case where a permeable spherical floc is placed in both a uniform and a simple shear flow field. Applying Darcy's law for permeability, Payatakes and Dassios [4] investigated a permeable spherical floc moving at a constant velocity toward a solid wall; a Beavers–Joseph–Saffman slip condition was assumed on the floc surface. Neale et al. [5] analyzed the movement of a swarm of permeable flocs by adopting a cell model. In a study of the sedimentation of a porous, spherical floc under the condition of creeping flow, Smith [6] assumed that a floc comprises several porous spherical particles, each wrapped by a fluid envelope. Veerapaneni and Wiesner [7] proposed a multilayer model where a floc is divided into several shells, each having a different permeability. Hsu and Hsieh [8] proposed using a two-layer model to simulate the behavior of a nonhomogeneous, porous, spherical floc in a flow field for Reynolds number ranging from 0.1 to 40.

The effect of the shape of a particle on its behavior in a creeping flow field was also discussed by many researchers. Brenner [9], for instance, analyzed the Stokes hydrodynamic resistance of a nonspherical particle immersed in an infinite medium under creeping flow. Blaser [10] evaluated the forces acting on the surface of a rigid, ellipsoidal particle

* Corresponding author.
E-mail address: jphsu@ccms.ntu.edu.tw (J.-P. Hsu).

0021-9797/03/$ – see front matter © 2003 Elsevier Science (USA). All rights reserved.
doi:10.1016/S0021-9797(02)00132-7

immersed in various flow fields, e.g., constant, simple shear, two-dimensional straining, and axisymmetric straining flow in the creeping flow region. Zlatanovski [11] investigated axisymmetric creeping flow past a porous prolate spheroidal particle. In all of these studies, the convection term in the Navier–Stokes equation was neglected, and an analytical solution was obtained.

In experimental research, Matsumoto and Suganuma [12] used a steel wool floc to investigate the effect of the permeability of a porous entity on its terminal velocity. Li and Ganczarczyk [13] examined experimentally the advection phenomenon within an activated sludge floc, which comprised a permeable outer layer and an impermeable core. They showed that while small flocs are impermeable, flocs with size from 100 to 500 μm are permeable, in general, and the transport mechanism inside them was of advective nature [14]. Lee et al. [2] found that the Reynolds number of the activated sludge floc obtained from a wastewater treatment plant of a bakery in a free-settling test ranged from 0.01 to 100, which implies that the Stokes law is inapplicable. Several problems concerned the movement of a permeable floc in a viscous fluid with a Reynolds number not in the creeping regime. Wu and Lee [15], for example, solved the problem where a porous, homogeneous sphere moving at a constant velocity in an infinite medium for Reynolds number ranged from 0.1 to 40. Wu and Lee [16] considered the problem in which a homogeneous porous sphere moved with a constant velocity toward an impermeable plate. Wu and Lee [17] considered the case where a porous, homogeneous sphere moved along the centerline of a cylindrical tube. The problem where a homogeneous, porous spheroidal floc moving at a constant velocity in an infinite medium for Reynolds number from 0.1 to 40 was studied by Wu and Lee [18].

In this study the previous result is extended to the case where the hydrodynamic force acts on a porous, nonhomogeneous spheroidal floc in a uniform flow field. A two-layer model is proposed to simulate the porous structure of a floc, and the effect of each layer on its behavior is investigated.

2. Theory

Referring to Fig. 1, we consider a spheroidal floc with a two-layer structure in an infinite fluid. Let a_1 and b_1 be respectively the polar and equatorial radii of the floc, and a_2 and b_2 be respectively the polar and equatorial radii of the inner layer. The symmetrical nature of the system under consideration suggests that a two-dimensional problem needs to be considered. Let the computational domain be characterized by length scales L and R, and let r and z be respectively the radial and the axial coordinates. The floc moves with a constant velocity $-\boldsymbol{V}$ and the surrounding fluid is fixed. For convenience, we assume that the floc remains fixed and the surrounding fluid flows with a constant bulk velocity $\boldsymbol{V}$.

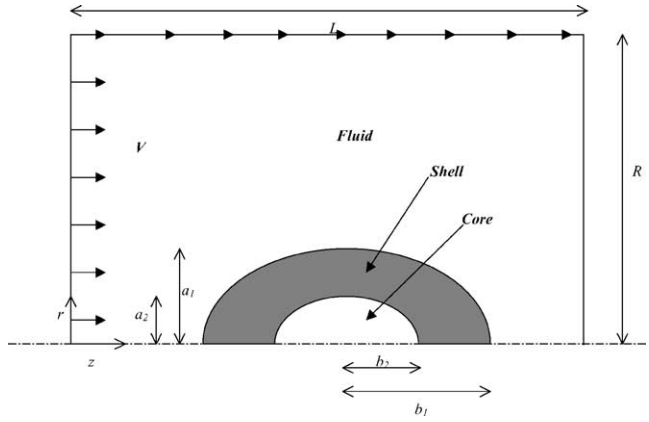

Fig. 1. Systematic representation of the problem considered. A floc of polar radius a_1 and equatorial radius b_1 comprises an inner layer of polar radius a_2 and equatorial radius b_2. L and R are the outer boundaries of the computation domain and r and z are coordinates.

We assume that the flow field in the liquid phase can be described by the Navier–Stokes equation [19]. In dimensionless form, we have

$$\mathbf{u}_f \cdot \nabla \mathbf{u}_f = \nabla P + \frac{1}{Re}\nabla^2 \mathbf{u}_f, \tag{1}$$

$$\nabla \cdot \mathbf{u}_f = 0. \tag{2}$$

In these expressions $Re = 2a_1 V\rho/\mu$ is the Reynolds number, ρ and μ being respectively the density and the viscosity of fluid; V is the magnitude of $\boldsymbol{V}$, P is the dimensionless pressure, ∇ is the dimensionless gradient operator, and $\mathbf{u}_f$ is the dimensionless velocity of fluid.

The Darcy–Brinkman model [5] and the continuity equation are adopted to describe the flow field inside a floc. In dimensionless form we have

$$\mathbf{u}_i + Re\frac{1}{\beta_i^2}\nabla P = \nabla^2 \mathbf{u}_i, \tag{3}$$

$$\nabla \cdot \mathbf{u}_i = 0. \tag{4}$$

In these expressions, β_i is the scaled radius of a floc defined by $a_1/\sqrt{k_i}$, k_i and $\mathbf{u}_i$ are respectively the permeability and the dimensionless velocity of fluid of region index i, and $i = 1$ and 2 represents respectively the outer and the inner layer of the floc.

The dimensionless boundary conditions associated with Eqs. (3) and (4) are assumed as

$$u_z = 1 \quad \text{as } r \to \infty, \tag{5a}$$

$$u_z = 1 \quad \text{as } z \to \infty, \tag{5b}$$

$$\frac{\partial \mathbf{u}_f}{\partial r} = \frac{\partial \mathbf{u}_1}{\partial r} = \frac{\partial \mathbf{u}_2}{\partial r} = 0, \quad r = 0, \tag{5c}$$

$$\mathbf{u}_f = \mathbf{u}_1 \quad \text{and} \quad \nabla \mathbf{u}_f = \nabla u_1 \tag{5d}$$

on the outer surface of outer layer,

$$\mathbf{u}_1 = \mathbf{u}_2 \quad \text{and} \quad \nabla \mathbf{u}_1 = \nabla \mathbf{u}_2 \tag{5e}$$

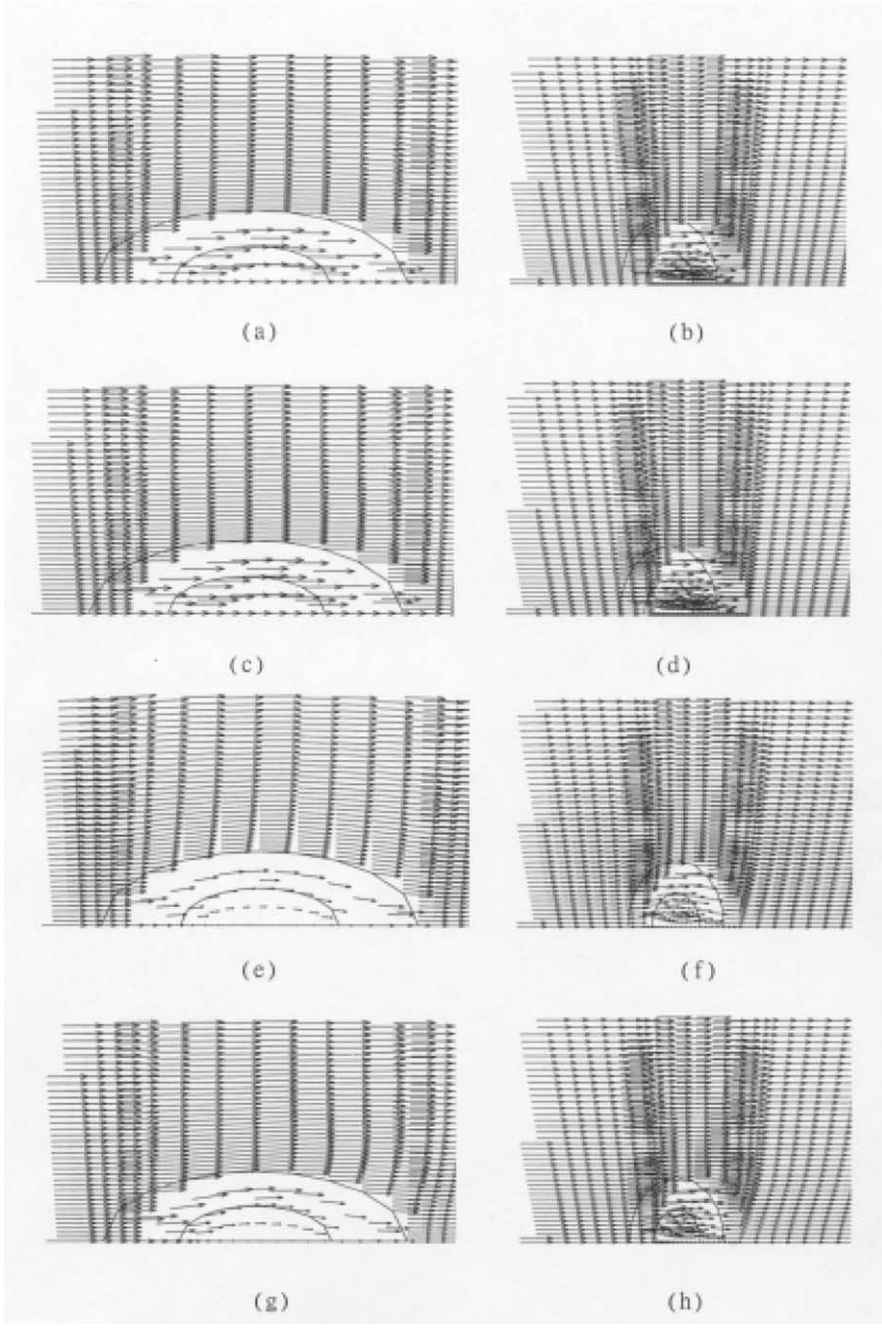

Fig. 2. Variation of velocity field for various combinations of a_1/b_1, k_1/k_2, and Re for the case where $A = 0.0113$ cm^2 and $\bar{\beta} = 0.6$. (a) $a_1/b_1 = 0.5$, $k_1/k_2 = 1$, and $Re = 0.1$; (b) $a_1/b_1 = 1.11$, $k_1/k_2 = 1$, and $Re = 0.1$; (c) $a_1/b_1 = 0.5$, $k_1/k_2 = 1$, and $Re = 40$; (d) $a_1/b_1 = 1.11$, $k_1/k_2 = 1$, and $Re = 40$; (e) $a_1/b_1 = 0.5$, $k_1/k_2 = 100$, and $Re = 0.1$; (f) $a_1/b_1 = 1.11$, $k_1/k_2 = 100$, and $Re = 0.1$; (g) $a_1/b_1 = 0.5$, $k_1/k_2 = 100$, and $Re = 40$; (h) $a_1/b_1 = 1.11$, $k_1/k_2 = 100$, and $Re = 40$.

on the outer surface of inner layer. In these expressions $\mathbf{u}_z$ is the dimensionless fluid velocity along z axis and u_z is the magnitude of $\mathbf{u}_z$.

The governing equations, Eqs. (1)–(4), and the associated boundary conditions, Eqs. (5a)–(5e), are solved numerically by FIDAP 8.6, commercial software (Fluid Dynamics Analysis Package) suitable for simulation of physical phenomena including fluid flow. It is based on a finite element method with bilinear four-node quadrilateral elements. The numbers of elements chosen for the fluid domain and the outer and the inner layers of a floc are 18,800, 35, and 30, respectively.

In summary, the key parameters that may influence the behavior of a floc include (i) $\bar{\beta}$, the volume-averaged radius, a measure connected to the volume-averaged permeability of a floc, which will be defined later, (ii) k_1/k_2, the ratio (permeability of outer layer/permeability of inner layer) for a floc, (iii) a_2/a_1, the ratio (radius of inner layer of

a floc/radius of floc), (iv) a_1/b_1, the ratio (polar radius/equatorial radius) for a floc, and (v) *Re*, the Reynolds number. These parameters will be discussed in the numerical simulation.

3. Results and discussion

Following the treatment of Neale et al. [5], the magnitude of the hydrodynamic drag force, F, acting on a homogeneous, porous nonspherical particle with a cross-sectional area A moving at speed V in an infinite fluid is calculated by

$$F = \left(\frac{1}{2}\rho V^2\right) A C_D \Omega, \quad \Omega \leqslant 1, \tag{6}$$

where C_D is the drag coefficient. The effect of the porous structure of the particle is taken into account by the correction factor Ω. For a nonporous particle, $\Omega = 1$. The drag coefficient of a nonporous sphere moving at a constant velocity, which is in the creeping flow regime, and the Reynolds number are related by [19]

$$C_D = \frac{24}{Re}. \tag{7}$$

For convenience, we define the volume-averaged permeability of a floc $\bar{k}$ and its volume-averaged radius $\bar{\beta}$ as

$$\bar{k} = \sum_{i=1}^{2} V_i k_i \Big/ \sum_{i=1}^{2} V_i, \tag{8}$$

$$\bar{\beta} = \frac{a_1}{\sqrt{\bar{k}}}. \tag{9}$$

The applicability of the numerical scheme adopted is examined by comparing the numerical result obtained with the analytic solution of Happel and Brenner [20] for the case of a rigid, spheroidal particle. The performance of the numerical scheme adopted is found to be satisfactory. For instance, at $Re = 0.1$ the maximum percentage deviation in $C_D\Omega$ for a_1/b_1 from 0.5 to 1.1 is less than 0.32%. Figure 2 shows the velocity field for various combinations of a_1/b_1, k_1/k_2 and *Re*, and the corresponding streamlines are presented in Fig. 3; both the behavior of a prolate spheroid ($a_1/b_1 = 0.5$) and that of an oblate spheroid ($a_1/b_1 = 1.11$) are examined. Both the cross-sectional area A and the scaled volume-averaged radius of a floc $\bar{\beta}$ are fixed in Figs. 2 and 3. Note that since a_1 is fixed in subsequent discussions, a constant volume-averaged radius of a floc $\bar{\beta}$ implies that the volume-averaged permeability of a floc is also constant. In Figs. 2a–2d and 3a–3d $k_1/k_2 = 1$; that is, the floc has a homogeneous structure. On the other hand, $k_1/k_2 = 100$ in Figs. 2e–2h and 3e–3h; that is, the inner part of the floc is much less permeable than its outer layer. Figure 2 reveals that, for a homogeneous floc, the velocity vectors inside are almost parallel to each other, regardless of its shape and the magnitude of *Re*. Also, the streamlines in the front part of the floc are symmetric to those in the rear part, as can be seen in Figs. 3a–3d. These results are consistent with those of Wu and Lee [18] in which nonspherical porous flocs are examined. The velocity field inside a nonuniform floc will be distorted by its inner (less permeable) part, regardless of its shape and the magnitude of *Re*, as can be seen in Figs. 2e–2h. Figures 3e and 3f indicate that if *Re* is small, the streamlines are symmetric, as in the case of homogeneous flocs. However, if *Re* is large, the streamlines become asymmetric, as shown in Figs. 3g and 3h. This is because if *Re* is large, wakes are formed in the rear part of a floc [20]. The deviation from a Stokes-law-like relation, i.e., $C_D\Omega$ is proportional to Re^{-1}, arises mainly from the convective flow of fluid. Since energy is consumed, the deviation is positive; that is, $C_D\Omega$ is greater than predicted by the Stokes-law-like relation. We conclude from Figs. 2 and 3 that the larger the difference between k_1 and k_2, the greater the difference in both velocity field and streamlines from those for the case $k_1 = k_2$ (homogeneous floc), even if the volume-averaged permeability is constant.

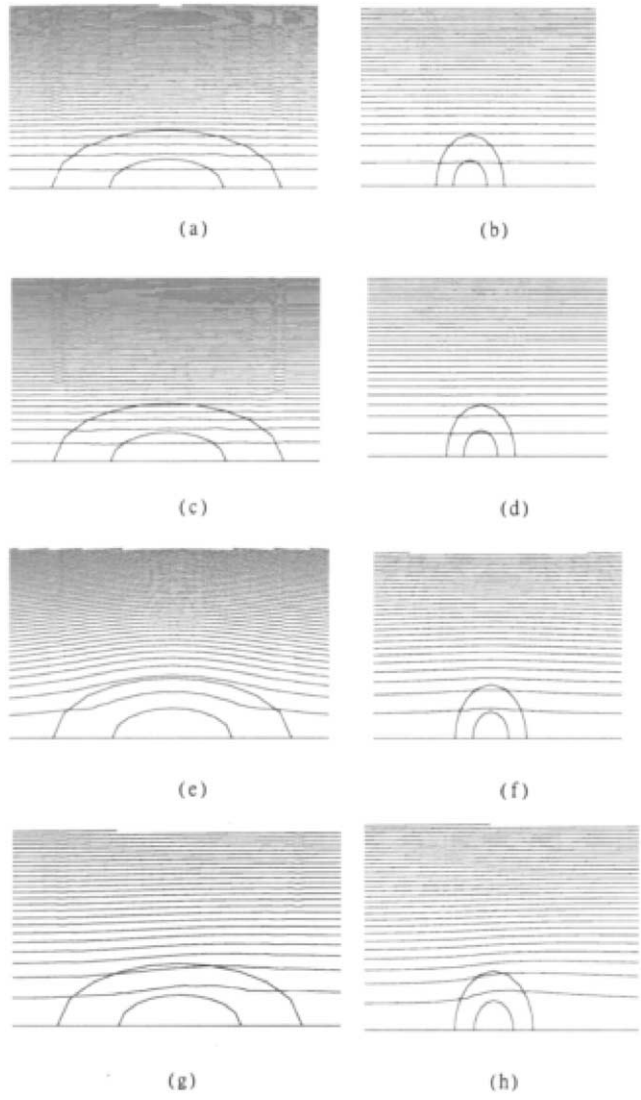

Fig. 3. Streamlines for the case of Fig. 2.

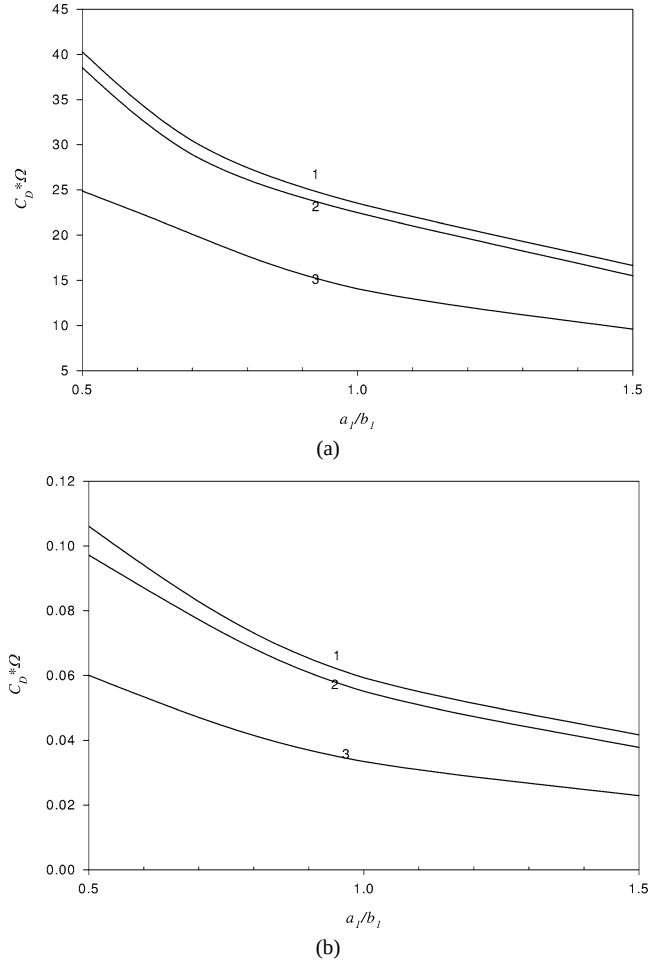

Fig. 4. Variation of $C_D\Omega$ as a function of a_1/b_1 for various k_1/k_2 and *Re* for the case when $\bar{\beta} = 0.6$. Curve 1, $k_1/k_2 = 8$; 2, $k_1/k_2 = 1/8$; 3, $k_1/k_2 = 1$. (a) $Re = 0.1$, (b) $Re = 40$.

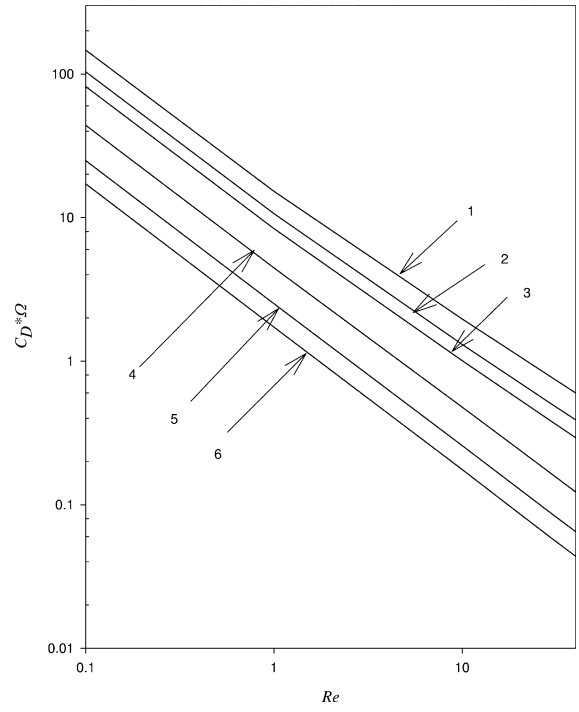

Fig. 5. Variation of $C_D\Omega$ as a function of *Re* for various combinations of a_1/b_1 and $\bar{\beta}$ for the case when $k_1/k_2 = 8$. $\bar{\beta} = 1.8$ in curves 1–3, and $\bar{\beta} = 0.6$ in curves 4–6. Curves 1 and 4, $a_1/b_1 = 0.5$; 2 and 5, $a_1/b_1 = 1$; 3 and 6, $a_1/b_1 = 1.11$.

3.1. Shape effect (a_1/b_1)

Figure 4 illustrates the variation of $C_D\Omega$ as a function of the shape parameter a_1/b_1 for various k_1/k_2 at two levels of *Re*. The polar radius of a floc, a_1, and therefore its cross-sectional area in the r-direction, A, are kept constant. As can be seen from Fig. 4, $C_D\Omega$ decreases with the increase in a_1/b_1. This is because for fixed a_1 the surface area of the floc decreases with the increase in a_1/b_1. For a homogenous floc at $Re = 0.1$, $C_D\Omega$ (prolate, $a_1/b_1 = 0.5$) $= 1.77C_D\Omega$ (sphere) and $C_D\Omega$ (sphere) $= 1.46C_D\Omega$ (oblate, $a_1/b_1 = 1.5$); and at $Re = 40$, $C_D\Omega$ (prolate, $a_1/b_1 = 0.5$) $= 1.71C_D\Omega$ (sphere) and $C_D\Omega$ (sphere) $= 1.41C_D\Omega$ (oblate, $a_1/b_1 = 1.5$). For a heterogeneous floc with $k_1/k_2 = 8$ at $Re = 0.1$, $C_D\Omega$ (prolate, $a_1/b_1 = 0.5$) $= 1.71C_D\Omega$ (sphere) and $C_D\Omega$ (sphere) $= 1.41C_D\Omega$ (oblate, $a_1/b_1 = 1.5$); and at $Re = 40$, $C_D\Omega$ (prolate, $a_1/b_1 = 0.5$) $= 1.79C_D\Omega$ (sphere) and $C_D\Omega$ (sphere) $= 1.43C_D\Omega$ (oblate, $a_1/b_1 = 1.5$). For a heterogeneous floc with $k_1/k_2 = 1/8$ at $Re = 0.1$, $C_D\Omega$ (prolate, $a_1/b_1 = 0.5$) $= 1.71C_D\Omega$ (sphere) and $C_D\Omega$ (sphere) $= 1.45C_D\Omega$ (oblate, $a_1/b_1 = 1.5$); and at $Re = 40$, $C_D\Omega$ (prolate, $a_1/b_1 = 0.5$) $= 1.76C_D\Omega$ (sphere) and $C_D\Omega$ (sphere) $= 1.46C_D\Omega$ (oblate, $a_1/b_1 = 1.5$). These imply that although the cross-sectional area of a floc is fixed, its $C_D\Omega$ still varies with its shape, regardless of the magnitude of *Re*. Since floc may assume various shapes in practice, knowing its exact shape can be important, and approximating it by an equivalent sphere may lead to significant deviation.

The variations of $C_D\Omega$ as a function of the Reynolds number *Re* for various combinations of a_1/b_1 and $\bar{\beta}$ for the case $k_1/k_2 = 8$ (i.e., the inner part of the floc is less permeable than its outer part) are presented in Fig. 5. Wu and Lee [18] concluded that, for the case of homogeneous floc with the same cross-sectional area, the drag force acting on a prolate is greater than that on an oblate. As can be seen in Fig. 5, this trend is also observed for the present nonhomogeneous floc. Under the conditions of Fig. 5, if $\bar{\beta} = 1.8$, the $C_D\Omega$ of a prolate is 41.7% greater than that of the corresponding spherical floc with $k_1/k_2 = 8$ at $Re = 0.1$ and 53.6% at $Re = 40$; the $C_D\Omega$ of an oblate is 21% smaller than that of the corresponding spherical floc at $Re = 0.1$ and 24.9% at $Re = 40$. If $\bar{\beta} = 0.6$, the $C_D\Omega$ of a prolate is 76.3% greater than that of the corresponding spherical floc with $k_1/k_2 = 8$ at $Re = 0.1$ and 89.2% at $Re = 40$; the $C_D\Omega$ of an oblate is 31.1% smaller than that of the corresponding spherical floc at $Re = 0.1$ and 32.8% at $Re = 40$. We conclude that the effect of the structure of a floc on $C_D\Omega$ is more significant at a higher *Re* and a larger volume-averaged permeability.

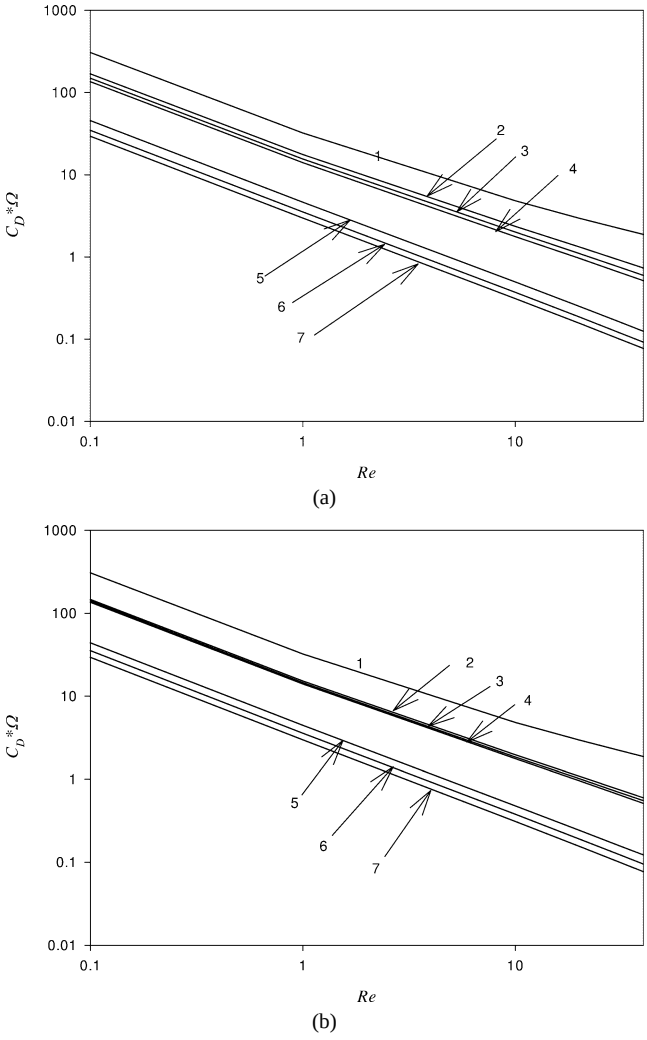

Fig. 6. Variation of $C_D\Omega$ as a function of *Re* for various k_1/k_2. (a) Curve 1, rigid particle (both k_2 and $k_1 \to 0$); 2 and 5, $k_1/k_2 = 1/8$; 3 and 6, $k_1/k_2 = 1/4$; 4 and 7, $k_1/k_2 = 1$. (b) Curve 1, rigid particle (both k_2 and $k_1 \to 0$); 2 and 5, $k_1/k_2 = 8$; 3 and 6, $k_1/k_2 = 4$; 4 and 7, $k_1/k_2 = 1$. Key: $a_1/b_1 = 0.5$, $\bar{\beta} = 1.8$ in curves 2–4, and $\bar{\beta} = 0.6$ in curves 5–7.

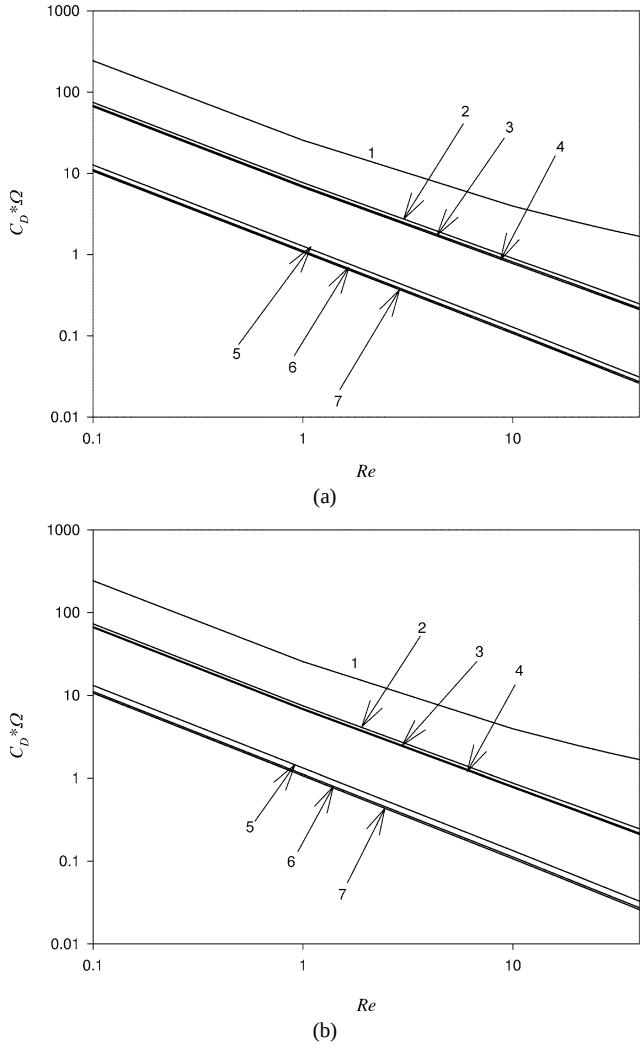

Fig. 7. Variation of $C_D\Omega$ as a function of *Re* for various k_1/k_2. (a) Curve 1, rigid particle (both k_2 and $k_1 \to 0$); 2 and 5, $k_1/k_2 = 1/8$; 3 and 6, $k_1/k_2 = 1/4$; 4 and 7, $k_1/k_2 = 1$. (b) Curve 1, rigid particle (both k_2 and $k_1 \to 0$); 2 and 5, $k_1/k_2 = 8$; 3 and 6, $k_1/k_2 = 4$; 4 and 7, $k_1/k_2 = 1$. Key: $a_1/b_1 = 1.11$, $\bar{\beta} = 1.8$ in curves 2–4, and $\bar{\beta} = 0.6$ in curves 5–7.

3.2. Effect of Reynolds number Re

The variations of $C_D\Omega$ as a function of Reynolds number *Re* at various k_1/k_2 for the case of a prolate floc with $k_2 > k_1$ (i.e., the inner layer is more permeable than the outer layer) are shown in Fig. 6a; those for the case $k_1 > k_2$ (i.e., the outer layer is more permeable than the inner layer) are illustrated in Fig. 6b. The results for the case of a rigid floc ($\bar{\beta} \to \infty$) are also presented in these figures for comparison. Both Figs. 6a and 6b suggest that the deviation of the $C_D\Omega$–*Re* relation from a Stokes-law-like relation is more pronounced for the case of a rigid floc. This is because at elevated *Re*, it is easier to see wakes behind a rigid floc than behind a porous floc [18]. For the case where a floc has a homogeneous structure ($k_1/k_2 = 1$), the larger the $\bar{\beta}$, the more serious is the deviation of the $C_D\Omega$–*Re* relation from the Stokes-law-like relation, as can be seen in both Figs. 6a and 6b. These figures also indicate that for a fixed volume-averaged permeability, the greater the deviation of k_1/k_2 from unity, the more apparent the deviation of the $C_D\Omega$–*Re* relation from the Stokes-law-like relation. According to Figs. 6a and 6b, if $\bar{\beta} = 1.8$ and $Re = 40$, the deviation from a Stokes-law-like relation for a homogeneous prolate floc is 52.7%; the deviation of a nonhomogeneous prolate floc is 64.5% if $k_1/k_2 = 8$, and is 81.5% if $k_1/k_2 = 1/8$. Figures 6a and 6b suggest that if the prolate floc is sufficiently porous ($\bar{\beta} = 0.6$), the deviation from the Stokes-law-like relation is inappreciable for $1/8 \leqslant k_1/k_2 \leqslant 8$ and *Re* up to 40. In this case, the more nonhomogeneous the structure of a floc the larger the $C_D\Omega$, and this effect is more pronounced as *Re* increases.

The variations of $C_D\Omega$ as a function of Reynolds number *Re* at various k_1/k_2 for the case of an oblate floc with $k_2 > k_1$ (i.e., the inner layer is more permeable than the outer layer) are shown in Fig. 7a; those for the case $k_1 > k_2$ (i.e., the outer

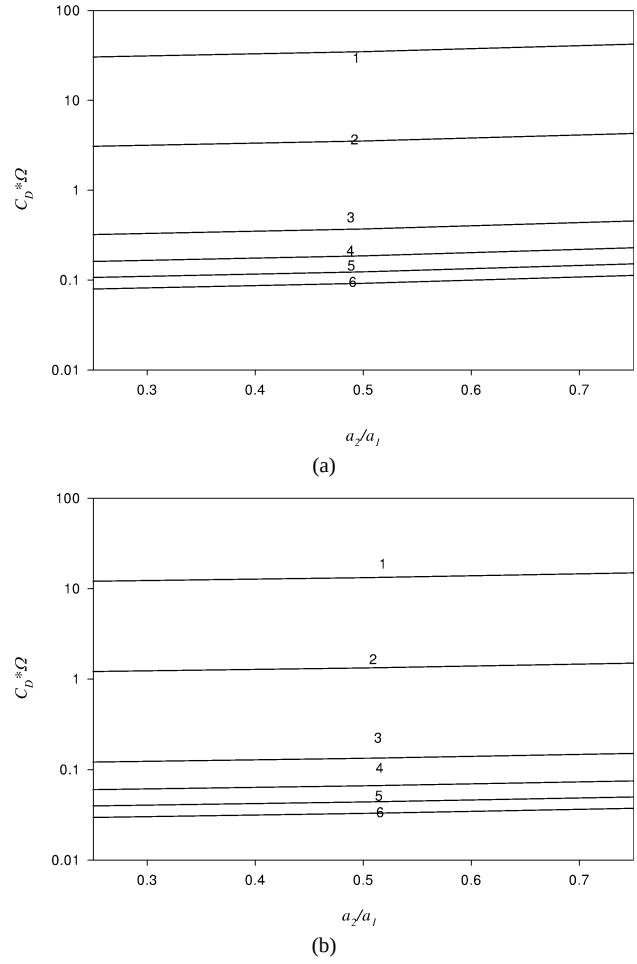

Fig. 8. Variation of $C_D\Omega$ as a function of a_2/a_1 for various *Re* for the case when $a_1/b_1 = 0.5$, $\bar{\beta} = 0.6$. (a) $k_1/k_2 = 4$. (b) $k_1/k_2 = 0.25$. Curve 1, $Re = 0.1$; 2, $Re = 1$; 3, $Re = 10$; 4, $Re = 20$; 5, $Re = 30$; 6, $Re = 40$.

layer is more permeable than the inner layer) are illustrated in Fig. 7b. For comparison, the corresponding results for the case of a rigid floc ($\bar{\beta} \to \infty$) are also presented in these figures. A comparison between Figs. 6a and 7a and between Figs. 6b and 7b reveals that, although the qualitative behavior of a prolate floc is similar to that of an oblate floc, there are some quantitative differences between the two. For example, if $\bar{\beta} = 1.8$ and $Re = 40$, the deviation from a Stokes-law-like relation for a homogeneous oblate is 36.5%; the deviation for a nonhomogeneous oblate with $k_1/k_2 = 1/8$ is 44.3%, and is 42.5% if $k_1/k_2 = 8$. These deviations are much lower than those for the corresponding prolate.

3.3. Effect of thickness ratio (a_2/a_1)

Figure 8a illustrates the variation of $C_D\Omega$ as a function of the ratio (a_2/a_1) for the case of a prolate floc with fixed $\bar{\beta}$ $(= 0.6)$ and outer layer more permeable than inner layer $(k_1/k_2 = 4)$ at various Reynolds numbers *Re*. That for the case where outer layer is less permeable than inner layer $(k_1/k_2 = 0.25)$ is presented in Fig. 8b. The qualitative behaviors of the curves shown in Fig. 8a are essentially the same as those shown in Fig. 8b. These include, for example, for fixed *Re* the larger the ratio (a_2/a_1) the larger the $C_D\Omega$, and for fixed (a_2/a_1), the larger the *Re* the larger the $C_D\Omega$. The former implies that, for a fixed volume-averaged permeability, $C_D\Omega$ increases with the size of the inner layer, regardless of whether it is less permeable than the outer layer or not. This can be explained by the variations of k_1 and k_2. For example, for the case of $\bar{\beta} = 0.6$, $a_1 = 0.12$ cm, and $k_1/k_2 = 0.25$, $\bar{k}$ is 0.04 cm^2, as calculated by Eq. (9). When a_2/a_1 is increased from 0.25 to 0.75, k_1 decreases from 0.0382 to 0.0177 cm^2 and k_2 decreases from 0.1528 to 0.0706 cm^2 accordingly. The simultaneous decrease in k_1 and k_2 as a_2/a_1 increases leads to an increase in $C_D\Omega$. For the case of $\bar{\beta} = 0.6$, $a_1 = 0.12$ cm, and $k_1/k_2 = 4$, $\bar{k}$ is 0.04 cm^2. As a_2/a_1 is increased from 0.25 to 0.75, k_1 increases from 0.0405 to 0.0585 cm^2 and k_2 increases from 0.01012 to 0.0146 cm^2. The simultaneous increase in k_1 and k_2 as a_2/a_1 increases also leads to an increase in $C_D\Omega$. This is because at $a_2/a_1 = 0.25$, since the volume of the inner layer is much smaller than that of the outer layer, the behavior of the floc is governed by the latter $(k_1 = 0.0405$ cm$^2)$. On the other hand, at $a_2/a_1 = 0.75$ its behavior is governed by its inner layer $(k_2 = 0.0146$ cm$^2)$.

4. Conclusions

In summary, the drag force experienced by a nonuniformly structured spheroidal floc in a uniform flow field is evaluated based on a two-layer model. We conclude that if the difference between the permeability of the outer layer of a floc and that of the inner layer is large, then both the velocity field and the streamlines are significantly different from those of the corresponding homogeneous floc, even if the volume-averaged permeability is constant. For a fixed volume-averaged permeability, the more nonhomogeneous a floc is the greater the drag force it experiences, regardless of whether its inner layer is less permeable than its outer layer or not. For the same cross-sectional area perpendicular to the flow direction, the drag force on a nonhomogeneous prolate floc is greater than that on a nonhomogeneous oblate floc. If the permeability of either the inner layer or the outer layer is sufficiently small, a positive deviation in the drag coefficient–Reynolds number relation from the Stokes-law-like relation can be observed. The deviation of a homogeneous porous prolate floc is more significant than that of a homogeneous porous oblate floc. For a fixed volume-averaged permeability and ratio (permeability of outer layer/permeability of inner layer), the drag coefficient increases with the size of the inner layer of a floc, regardless of whether the inner layer is less permeable than that of the outer layer or not.

Acknowledgment

This work is supported by the National Science Council of the Republic of China.

References

[1] D.H. Li, J. Ganczarczyk, Biotechnol. Bioeng. 35 (1990) 57.
[2] D.J. Lee, G.W. Chen, Y.C. Liao, C.C. Hsieh, Water Res. 30 (1996) 541.
[3] P.M. Adler, J. Colloid Interface Sci. 81 (1981) 531.
[4] A.C. Payatakes, G. Dassias, Chem. Eng. Sci. 58 (1987) 119.
[5] G. Neale, N. Epstein, W. Nader, Chem. Eng. Sci. 28 (1973) 1865.
[6] T.N. Smith, Chem. Eng. Sci. 53 (1998) 315.
[7] S. Veerapaneni, M.R. Wiesner, J. Colloid Interface Sci. 177 (1996) 45.
[8] J.P. Hsu, Y.H. Hsieh, Chem. Eng. Sci. 57 (2002) 2627.
[9] H. Brenner, Chem. Eng. Commun. 148 (1996) 487.
[10] S. Blaser, Chem. Eng. Sci. 57 (2002) 515.
[11] T. Zlatanovski, Quart. J. Appl. Math. 52 (1999) 111.
[12] K. Matsumoto, A. Suganuma, Chem. Eng. Sci. 32 (1977) 445.
[13] D.H. Li, J. Ganczarczyk, Water Res. 22 (1988) 789.
[14] D.H. Li, J. Ganczarczyk, Water Environ. Res. 64 (1992) 236.
[15] R.M. Wu, D.J. Lee, Water Res. 32 (1998) 760.
[16] R.M. Wu, D.J. Lee, Chem. Eng. Sci. 53 (1998) 3571.
[17] R.M. Wu, D.J. Lee, Chem. Eng. Sci. 54 (1999) 5717.
[18] R.M. Wu, D.J. Lee, Water Res. 35 (2001) 3226.
[19] R.B. Bird, W.E. Stewart, E.N. Lightfoot, Transport Phenomena, Wiley, New York, 1960.
[20] J. Happel, H. Brenner, Low Reynolds Number Hydrodynamics, Academic Press, New York, 1983.